


CLINICAL STUDY



Identification of serum biomarkers for chronic kidney disease using serum metabolomics

Xi Gu^a, Yindi Dong^a, Xuemei Wang^{b,c}, Zhigang Ren^{b,c}, Guanhua Li^a, Yaxin Hao^a, Jian Wu^d, Shiyuan Guo^e, Yajuan Fan^f, Hongyan Ren^g, Chao Liu^g, Suying Ding^h, Weikang Li^h, Ge Wu^a  and Zhangsuo Liu^a

^aDepartment of Nephrology, The First Affiliated Hospital of Zhengzhou University, Zhengzhou, China; ^bDepartment of Infectious Diseases, the First Affiliated Hospital of Zhengzhou University, Zhengzhou, China; ^cGene Hospital of Henan Province, Precision Medicine Center, the First Affiliated Hospital of Zhengzhou University, Zhengzhou, China; ^dCollege of Public Health, Zhengzhou University, Zhengzhou, China; ^eDepartment of Nephrology, Xinxiang Central Hospital, Xinxiang, China; ^fDepartment of Nephrology, Zhumadian Central Hospital, Zhumadian, China; ^gShanghai Mobio Biomedical Technology Co., Ltd, Shanghai, China; ^hHealth Management Center, the First Affiliated Hospital of Zhengzhou University, Zhengzhou, China

ABSTRACT

This study aimed to identify biomarkers for chronic kidney disease (CKD) by studying serum metabolomics. Serum samples were collected from 194 non-dialysis CKD patients and 317 healthy controls (HC). Using ultra-high-performance liquid chromatography-tandem mass spectrometry (UPLC-MS), untargeted metabolomics analysis was conducted. A random forest model was developed and validated in separate sets of HC and CKD patients. The serum metabolomic profiles of patients with chronic kidney disease (CKD) exhibited significant differences compared to healthy controls (HC). A total of 314 metabolites were identified as significantly different, with 179 being upregulated and 135 being downregulated in CKD patients. KEGG enrichment analysis revealed several key pathways, including arginine biosynthesis, phenylalanine metabolism, linoleic acid metabolism, and purine metabolism. The diagnostic efficacy of the classifier was high, with an area under the curve of 1 in the training and validation sets and 0.9435 in the cross-validation set. This study provides comprehensive insights into serum metabolism in non-dialysis CKD patients, highlighting the potential involvement of abnormal biological metabolism in CKD pathogenesis. Exploring metabolites may offer new possibilities for the management of CKD.

ARTICLE HISTORY

Received 2 January 2024
Revised 28 July 2024
Accepted 21 September 2024

KEYWORDS

Chronic kidney disease;
serum metabolomics;
metabolic pathways;
biomarkers; gut
microbiome


Introduction

Chronic kidney disease (CKD) is a heterogeneous group of diseases that irreversibly change the function and structure of the kidneys [1]. In 2017, the global prevalence of CKD was 9.1%, representing 697.5 million patients, including 132.3 million in China [2]. CKD has an insidious onset, and its cause is complex and uncertain. Age, sex, genetics, autoimmunity, exposure to heavy metals, smoking, excessive drinking, viral infections, obesity, hypertension, and diabetes are risk factors for CKD. Still, prevention strategies based on traditional risk factors such as hypertension, blood glucose management, and obesity do not reduce the prevalence of CKD [3]. Glomerular loss and hypertrophy, impaired glomerular filtration rate, and renal fibrosis are part of the pathophysiological process of CKD [4], but our understanding of the pathophysiology of CKD remains limited.

The loss of kidney function in CKD is progressive and irreversible, eventually leading to end-stage renal disease (ESRD), with many complications, high mortality, and a large economic burden. There is a lack of targeted treatment measures for end-stage renal disease, and the present treatment strategies mainly rely on renal replacement therapy, including dialysis and kidney transplantation. It is estimated that by 2040, the number of deaths due to CKD may increase to 2.2 million or even 4 million [2].

Currently, urine protein excretion, renal histopathology, serum creatinine (SCr), and estimated glomerular filtration rate (eGFR) are commonly used to diagnose CKD, but these methods have poor sensitivity and have limited value in the early detection of kidney injury. SCr is used to stage CKD [5], but it varies with age, race, sex, muscle mass, total body weight, and nutritional status [6]. The available biomarkers are limited, and there is an urgent need to find novel

CONTACT Ge Wu  fccwug@zzu.edu.cn; Zhangsuo Liu  zhangsuoliu@zzu.edu.cn  No. 1 Jianshe East Road, Erqi District, Zhengzhou City, Henan Province

 Supplemental data for this article can be accessed online at <https://doi.org/10.1080/0886022X.2024.2409346>.

© 2024 The Author(s). Published by Informa UK Limited, trading as Taylor & Francis Group

This is an Open Access article distributed under the terms of the Creative Commons Attribution-NonCommercial License (<http://creativecommons.org/licenses/by-nc/4.0/>), which permits unrestricted non-commercial use, distribution, and reproduction in any medium, provided the original work is properly cited. The terms on which this article has been published allow the posting of the Accepted Manuscript in a repository by the author(s) or with their consent.

biomarkers that are more specific and sensitive to enable the timely and accurate detection of CKD and to find new therapeutic targets [7–9].

The kidneys influence the levels of circulating low-molecular-weight metabolites through glomerular filtration, tubular secretion, reabsorption, catabolism, and biosynthesis. Hence, abnormal renal function can affect the levels of various metabolites in the blood [10]. Metabolomics is the study of all metabolites in a given system and can be used to identify the changes that occur in a disease and metabolites that could be used as biomarkers for screening, diagnosis, and/or monitoring [11]. Metabolomics, especially the untargeted type, constitutes one of the most frequently applied approaches in biological research, and it aims to measure the comprehensive metabolomic profiles in various biological samples under both normal physiological as well as pathophysiological conditions. The metabolomics approach has been used to study various diseases, including kidney diseases [12], Marfan syndrome [13], diabetic retinopathy [14], and diabetic nephropathy [15]. Still, predictive biomarkers for the early detection of CKD remain to be identified.

Therefore, this study aimed to examine the serum metabolomics of patients with CKD, explore the possible pathogenesis of CKD, and seek biomarkers of CKD. The results could help prevent, detect, and manage CKD.

Materials and methods

Study design and participants

This study was conducted according to the tenets of the Declaration of Helsinki and the Conference for Coordination of Clinical Practice. The study was reviewed and approved by the Institutional Review Board of the First Affiliated Hospital of Zhengzhou University (# 2021-KY-0655). All participants signed written informed consent after the study protocol was fully explained.

Data collection was conducted at the time of specimen collection. The specimens were collected in the Zhengzhou and Hangzhou areas in 2018 and 2019. The demographic and clinical data of participants were obtained from questionnaires and hospital electronic medical records of hospitals. Metabolomics was performed once all specimens were collected.

The diagnosis and staging of all patients with CKD were based on the criteria described in the KDIGO 2020 clinical practice guideline for evaluating and managing CKD [16]. The participants were staged according to eGFR (mL/min/1.73 m²): CKD1 (eGFR ≥90), CKD2 (eGFR 60–89), CKD3 (eGFR 45–59), CKD4 (eGFR 15–44), and CKD 5 (eGFR <15) [16]. The Cockcroft-Gault(CG) formula was used to eGFR.

$$eGFR = \frac{(140 - \text{age}) \times (\text{wtkg})}{72 \times \text{Scr}(\text{mg/dl})} \quad (15\% \text{ less in females}).$$

The exclusion criteria were (1) <18 or >80 years of age, (2) a CKD-related drug therapy had been initiated, or the candidate had undergone hemodialysis, peritoneal dialysis, or kidney transplantation, (3) any serious disease of the digestive system, blood, or respiratory system or a tumor, or (4) missing essential clinical information.

The control group comprised healthy volunteers who visited the hospital for their annual physical examination. The inclusion criteria were (1) they match the basic characteristics of the CKD group, except for CKD, (2) no diseases of the urinary system, blood system, endocrine system, digestive system, etc., and (3) a history of regular physical examination at the hospital.

Specimen collection

The specimens (5 mL of venous blood) were collected early in the morning after an overnight fast (Disposable BD serum collection tube, no additives). The blood was centrifuged at 3000 rpm for 10 min, and 500 µL of supernatant was stored at –80 °C for testing.

Metabolite extraction

The metabolites were extracted from 100 µL of serum using 400 µL of methanol: water (4:1, v/v) with 0.02 mg/mL L-2-chlorophenyl alanine as the internal standard. The mixture was allowed to settle at –10 °C and treated in a high-throughput tissue crusher Wonbio-96c (Shanghai Wanbo Biotechnology Co., Ltd) at 50 Hz for 6 min and then by ultrasound at 40 kHz for 30 min at 5 °C. The samples were placed at –20 °C for 30 min to allow the proteins to precipitate. After centrifugation at 13,000 ×g at 4 °C for 15 min, the supernatant was carefully transferred to sample vials for UPLC-MS/MS analysis.

Quality control sample

A pooled quality control (QC) sample was prepared by mixing equal volumes of all specimens. The QC samples were disposed of and tested in the same manner as the analytical samples. The QC sample was injected every 10 samples to monitor the stability of the analysis.

Chromatographic separation of the metabolites

The chromatographic separation of the metabolites was performed on a Thermo UHPLC system equipped with an ACQUITY UPLC HSS T3 column (100 × 2.1 mm i.d., 1.8 µm; Waters, Milford, USA). The samples (2 µL) were separated using the HSS T3 chromatographic column and detected by mass spectrometry. Mobile phase A consisted of 95% water + 5% acetonitrile (containing 0.1% formic acid). Mobile phase B consisted of 47.5% acetonitrile + 47.5% isopropyl alcohol + 5% water (containing 0.1% formic acid). At 0–3.5 min, mobile phase B increased from 0% to 24.5%, and the flow rate was 0.40 mL/min. At 3.5–5 min, mobile phase B increased from 24.5% to 65%, and the flow rate was 0.40 mL/min. At 5–5.5 min, mobile phase B increased from 65% to 100%, and the flow rate was 0.40 mL/min. At 5.5–7.4 min, mobile phase B was maintained at 100%, and the flow rate increased from 0.40 to 0.60 mL/min. At 7.4–7.6 min, mobile phase B decreased from 100% to 51.5%, and the flow rate was 0.6 mL/min. At

7.6–7.8 min, mobile phase B decreased from 51.5% to 0%, and the flow rate decreased from 0.6 to 0.5 mL/min. At 7.8–9 min, 0% of mobile phase B was maintained, and the flow rate decreased from 0.5 to 0.4 mL/min. At 9–10 min, 0% mobile phase B was maintained, and the flow rate was 0.4 mL/min. The column temperature was 40°C.

Mass spectrometry

The mass spectrometric data were collected using a Thermo UHPLC-Q Exactive HF-X Mass Spectrometer equipped with an electrospray ionization (ESI) source operating in either the positive or negative ion mode. The positive and negative ion scanning mode was adopted to collect the sample quality spectrum signal. The quality scanning range was m/z 70–1050. The parameters were ion spray voltage, positive ion voltage 3500 V, negative ion voltage 2800 V, sheath gas 40 psi, auxiliary heating gas 10 psi, ion source heating temperature 400°C, 20–40–60 V cyclic collision energy, MS1 resolution 70,000, and MS2 resolution 17,500.

Data analysis and data preprocessing

After the UPLC-MS analysis, the raw data were imported into Progenesis Q1 2.3 (Nonlinear Dynamics, Waters, USA) for peak detection and alignment. The preprocessing generated a data matrix that consisted of the retention time (RT), m/z values, and peak intensity. The data matrix used the 80% rule to remove the missing value, i.e. the variables with non-zero values above 80% in at least one group of samples were retained, and then the vacant value was filled (the minimum value in the original matrix fills the vacancy value). After filtering, the minimum metabolite values were imputed for specific samples for which the metabolite levels fell below the lower limit of quantification, and each metabolic feature was normalized by sum. As an internal standard for data QC (reproducibility), the metabolomic features for which the relative standard deviation (RSD) was $QC > 30\%$ were discarded. Following normalization procedures and imputation, statistical analysis was performed on log-transformed data to identify the significant differences in metabolite levels between groups. The mass spectra of these metabolomic features were identified using the accurate mass, MS/MS fragments spectra, and isotope ratio difference and by searching in reliable biochemical databases such as the Human Metabolome Database (HMDB) (<http://www.hmdb.ca>) and the METLIN database (<https://metlin.scripps.edu>). The mass tolerance between the measured m/z values and the exact mass of the components of interest was ± 10 ppm. For metabolites having MS/MS confirmation, only the ones with an MS/MS fragments score of > 30 were considered as confidently identified.

Differential metabolite analysis

The metabolic profiles of the serum samples were compared between CKD and HC using univariable and multivariable analyses. Variable distribution was normalized using log

transformation for all preprocessed data. The Mann–Whitney–Wilcoxon test with a false discovery rate correction was used to measure the significance of each metabolite. A multivariable statistical analysis was performed using the R software package (ropis) (version 1.6.2, <http://bioconductor.org/packages/release/bioc/html/ropis.html>) from Bioconductor. The principal component analysis (PCA) using an unsupervised method was used to examine the intrinsic variation within the dataset and obtain an overview of the variation between groups, and visualize the general clustering, trends, and outliers. All metabolite variables were scaled to unit variances before conducting the PCA. A supervised partial least squares discrimination analysis (PLS-DA) and orthogonal partial least squares discriminate analysis (OPLS-DA) were done to determine the overall differences in the metabolomic profiles of the groups and find the differential metabolites between groups. Compared with PLS-DA, OPLS-DA can effectively reduce the complexity of a model and enhance the interpretation ability without compromising the prediction ability of the model to check the differences between groups to the greatest extent. In order to prevent model overfitting, 200 permutation tests were used to investigate the fitting effect of the model. Generally, if the Q^2 intercept value was < 0 or the Q^2 values were lower on the left side of the permutation test chart than the original point on the right, the fitness of the model was considered better.

The models were trained on 80% subsets with tenfold cross-validation repeated three times. The 20% holdout subsets were used to validate the final model. Each training iteration was repeated ten times per model per cause. The hyperparameters were manually set to favor a more generalizable model and limit overfitting. Models were assessed with four evaluation metrics to account for how the skewed distribution of CKD causes might overestimate model performance: receiver-operator area-under-the-curve (ROC-AUC), precision-recall area-under-the-curve (PR-AUC), F1 score, and Matthews correlation coefficient (MCC). Significant features were designated as metabolites included in the top 10% most-weighted features in $\geq 5/10$ training iterations.

The potential metabolites between the CKD and HC groups were identified based on the variable importance in the projection (VIP) calculated in the OPLS-DA model, and the metabolites with $VIP > 1.0$ were selected. A panel of potential metabolites responsible for the differences between CKD and HC was obtained. Fold change (FC) was calculated based on mean ratios for CKD/HC. The differential metabolites between CKD and HC were identified using Student's t -test with a threshold of $p < 0.05$ in SPSS 22.0 (IBM, Armonk, NY, USA). Metabolites with multivariable and univariable statistical significance ($VIP > 1$ and $p < 0.05$) were considered potential biomarkers.

Molecular pathway identification

By integrating the relevant information from HMDB, Kyoto Encyclopedia of Genes and Genomes (KEGG) (<http://www.kegg.com>) compound database, and the Lipid Metabolites and Pathways Strategy (LIPID MAPS) database (<http://www.lipidmaps.org>).

lipidmaps.org), the pathway annotation analysis of the differential metabolites was performed. The metabolic pathway map was obtained (except for the metabolites that were not found). After obtaining the KEGG ontology of the metabolites, according to the KEGG level (KEGG BRITE) database, the KEGG results were divided into four levels, denoted by A, B, C, and D, respectively, and the level was incremented once. BRITE A contained six branches, including cellular processes, environmental information processing, genetic information processing, human diseases, metabolism, and organismal systems. BRITE B belonged to a small branch within BRITE A. BRITE C was a specific metabolic pathway. BRITE D was a single metabolite. These metabolites were classified according to the pathways they were involved in or the functions they performed. The KEGG pathway topology was mainly based on each cyclic reaction structure, combined with the relative position of the biomolecules and a method of evaluating the relative importance of pathways through weighted scores. In order to compare the different pathways, the comprehensive score of each pathway was standardized to 1. The importance of each metabolite was measured according to its relative position importance to obtain a weighted score, which was obtained by calculating the weighted score of matching metabolites and the cumulative importance score of the current channel. The higher the score, the greater the influence of the channel.

Random forest modeling

Random forest modeling was used to determine the best predictive model for CKD [17].

Predictive value of the biomarkers

In order to identify the biological processes most related to CKD, a channel enrichment analysis was carried out using Fisher's exact test. The receiver operating characteristic (ROC) curve analysis was performed using the survival analysis module to evaluate the area under the curve (AUC) and to compare the diagnostic ability of significantly different metabolites between the two groups.

Statistical analysis

The continuous variables were presented as means \pm standard deviations or median (interquartile ranges). The categorical variables were presented as n (%). Differences between the two groups were detected using Student's t -test for normal continuous variables, the Wilcoxon rank-sum test for non-normal continuous variables, and the chi-square test or Fisher's exact test for categorical variables. Statistical analyses were performed using SPSS 21.0 for Windows (IBM, Armonk, NY, USA). Statistical significance was defined as $p < 0.05$. Data transformation, normalization, or evaluation of outliers was not used in the study.

Results

Specimen selection

This study collected 529 serum specimens, but 512 met the eligibility criteria (194 from patients with CKD and 317 from healthy controls (HC). The samples from Zhengzhou were randomly divided into the training and verification sets (Figure 1). In the training set, the serum metabolomics of 210 HC and 110 CKD patients were determined, the key serum markers were identified, and a CKD classifier was constructed using a random forest model. In the validation set, the diagnostic efficacy of the CKD classifier was validated in 35 CKD patients and 107 HC. Finally, the independent diagnostic power of the CKD classifier was also confirmed in the 49 CKD patients from Hangzhou. Table 1 presents the characteristics of the participants.

Metabolic profiles and multivariable analysis

UPLC-MS detected 25,291 variables among the 512 participants, including 14,669 positive and 10,622 negative ion modes. After preprocessing the original data, a data matrix containing retention time, mass-nucleus ratio, peak intensity, chemical formula, and metabolite number was obtained, in which 597 positive ion modes and 494 negative ion modes were identified (Online Supplementary Data S1).

In order to evaluate the systemic changes of the metabolome in CKD and identify biomarkers, PCA, PLS-DA, and OPLS-DA were performed on the serum metabolites from CKD patients and HC. The PCA score plots showed that the metabolic pattern differs for CKD patients and HC. The PLS-DA and OPLS-DA score plots could be readily divided into two clusters, indicating that the serum metabolic pattern was significantly altered in the participants with CKD. The QC samples were intensively distributed with good repeatability, indicating that the system was stable (Figure 2). Hence, the PCA score plots showed that the metabolic pattern was different between the CKD and HC groups. In addition, the PLS-DA and OPLS-DA score plots could be readily divided into two distinct clusters, indicating that the serum metabolic pattern was significantly altered in CKD.

Selection of differential metabolites

Using the VIP values ($VIP > 1$) derived from the OPLS-DA and the P -values ($p < 0.05$), 314 differential metabolites were identified to be specific for CKD (Online Supplementary Data S2). The heatmap (Figure S1 and Online Supplementary Data S2) shows the relative intensities of these identified metabolites. Through cluster analysis of all the identified metabolites, the high and low expressions were crossed together. The expression patterns of 210 HC samples were similar, and the expression patterns of 110 CKD samples were also similar. The metabolites whose expression was upregulated in CKD were downregulated in HC, and those whose expression was upregulated in HC were down-regulated in CKD (Figure S1

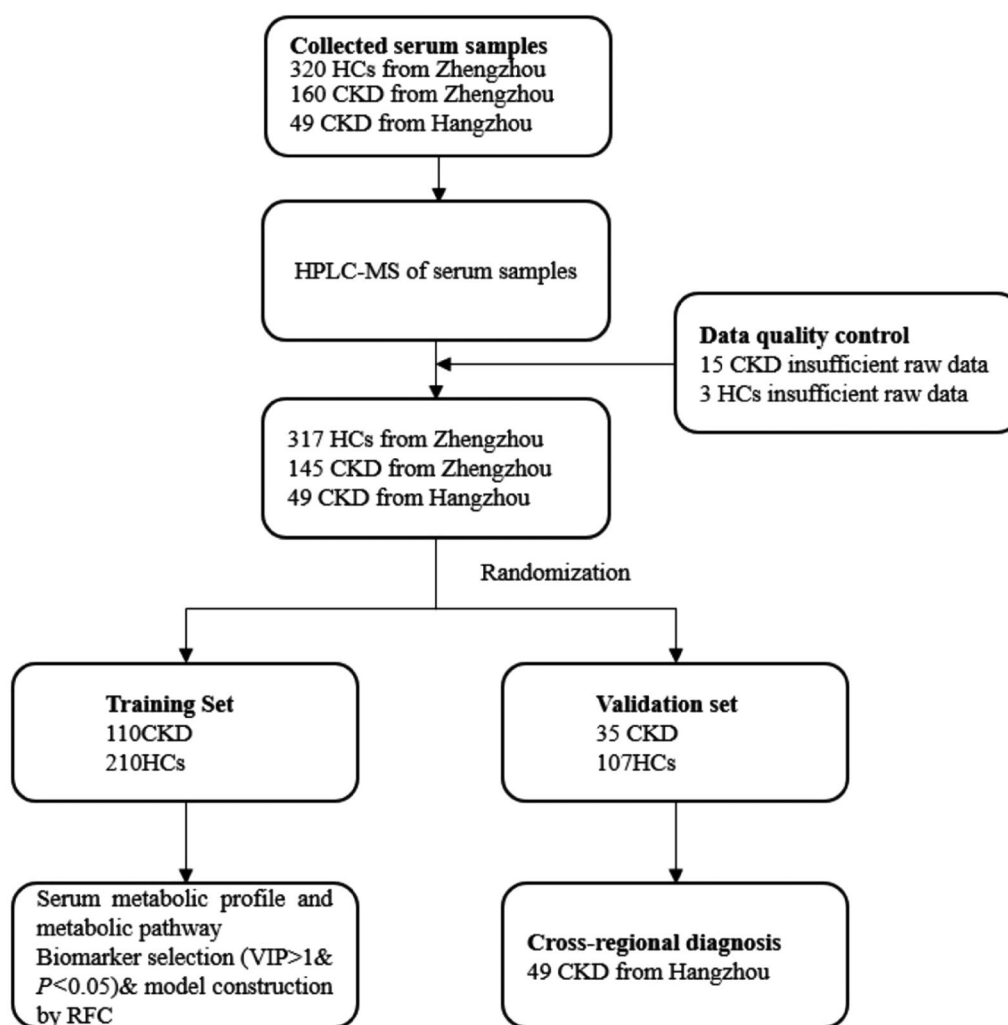


Figure 1. Study design and participant flowchart. CKD: chronic kidney disease; HCs: healthy controls; UPLC-MS: Ultra-high-performance liquid chromatography-tandem mass spectrometry; VIP: variable importance in the projection; *P*: *P* value; RFC: random Forest classifier model.

Table 1. Clinical characteristics of participants in the discovery and validation set.

Clinical indices	Discovery set (n=320)			Validation set (n=142)		
	HC (n=210)	CKD (n=110)	P	HC (n=107)	CKD (n=35)	P
Age (years)	47 (43,54)	53 (44,63)	0.073	49 (44,55)	46 (41,64)	0.533
Sex (female/male)	143/67	70/40	0.422	42/65	14/21	0.937
WBC (×10 ⁹ /L)	6.01 (5.2,7.1)	6.23 (4.90,8.13)	0.302	6.23 ± 1.61	6.81 ± 2.38	0.669
RBC (×10 ¹² /L)	4.85 (4.50,5.15)	3.70 (2.99,4.31)	<0.001	4.73 ± 0.40	3.68 ± 0.73	<0.001
Hb (g/L)	151.5 (139.1,159.0)	111 (90.75,132.63)	<0.001	146.45 ± 15.22	113.83 ± 26.02	<0.001
PLT (×10 ⁹ /L)	234.43 ± 52.04	208.31 ± 75.45	<0.001	231.97 ± 57.35	209.91 ± 61.32	0.225
Ca (mmol/L)	2.39 (2.33,2.45)	2.21 (2.08,2.32)	<0.001	2.38 (0.12)	2.16 (0.23)	<0.001
P (mmol/L)	1.13 (1.02,1.22)	1.26 (1.09,1.72)	<0.001	1.2 (0.24)	1.28 (0.37)	<0.001
BUN (mmol/L)	4.61 (3.83,5.51)	15.00 (7.40,24.85)	<0.001	4.56 (1.61)	12.7 (16.3)	<0.001
SCr (μmol/L)	69.8 ± 13.22	406.55 ± 123.85	<0.001	67.31 ± 13.06	363.69 ± 133.65	<0.001
UA (μmol/L)	317.64 ± 80.40	406.55 ± 123.85	<0.001	302 (250,360)	346 (284,416)	0.18
FBG (mmol/L)	5.32 (5.04,5.80)	4.74 (4.32,5.27)	<0.001	5.36 (5.09,6.00)	4.63 (4.32,5.05)	<0.001
ALB (g/L)	47.67 ± 2.40	37.69 ± 8.04	<0.001	47.63 ± 2.76	36.98 ± 8.79	<0.001
TC (mmol/L)	4.75 ± 0.86	4.85 ± 1.98	0.481	4.84 (4.15,5.18)	5.09 (4.01,5.83)	0.512
TG (mmol/L)	1.35 (0.94,1.90)	1.43 (1.01,2.16)	0.25	1.40 (0.96,1.82)	1.59 (1.07,2.21)	0.566
LDL (mmol/L)	2.95 (2.41,3.41)	2.92 (2.11,3.76)	<0.001	2.95 ± 0.76	3.32 ± 1.45	0.338
24-h UTP (g)	ND	1.78 (0.68,4.79)		ND	2.86 (0.85,5.33)	
CKD clinical stage	Stages 1-2	28 (25.45%)			11 (31.43%)	
	Stages 3-4	33 (30.00%)			12 (34.29%)	
	Stage 5	49 (44.55%)			12 (34.29%)	

Continuous variables were expressed as means ± standard deviations or median (interquartile ranges). Categorical variables were expressed as percentages. Continuous variables were compared using Student's *t*-test or Wilcoxon rank-sum test, and categorical variables were compared using the chi-square test or Fisher's exact test.

CKD: chronic kidney disease; HC: healthy control; WBC: white blood cells; RBC: red blood cells; Hb: hemoglobin; PLT: platelet; Ca: calcium; BUN: blood Urea nitrogen; SCr: serum creatinine; UA: uric acid; FBG: fasting blood glucose; ALB: albumin; TC: total cholesterol; TG: triglyceride; LDL: low-density lipoprotein; 24-h UTP: 24-h urine protein quantitation; ND: no detection.

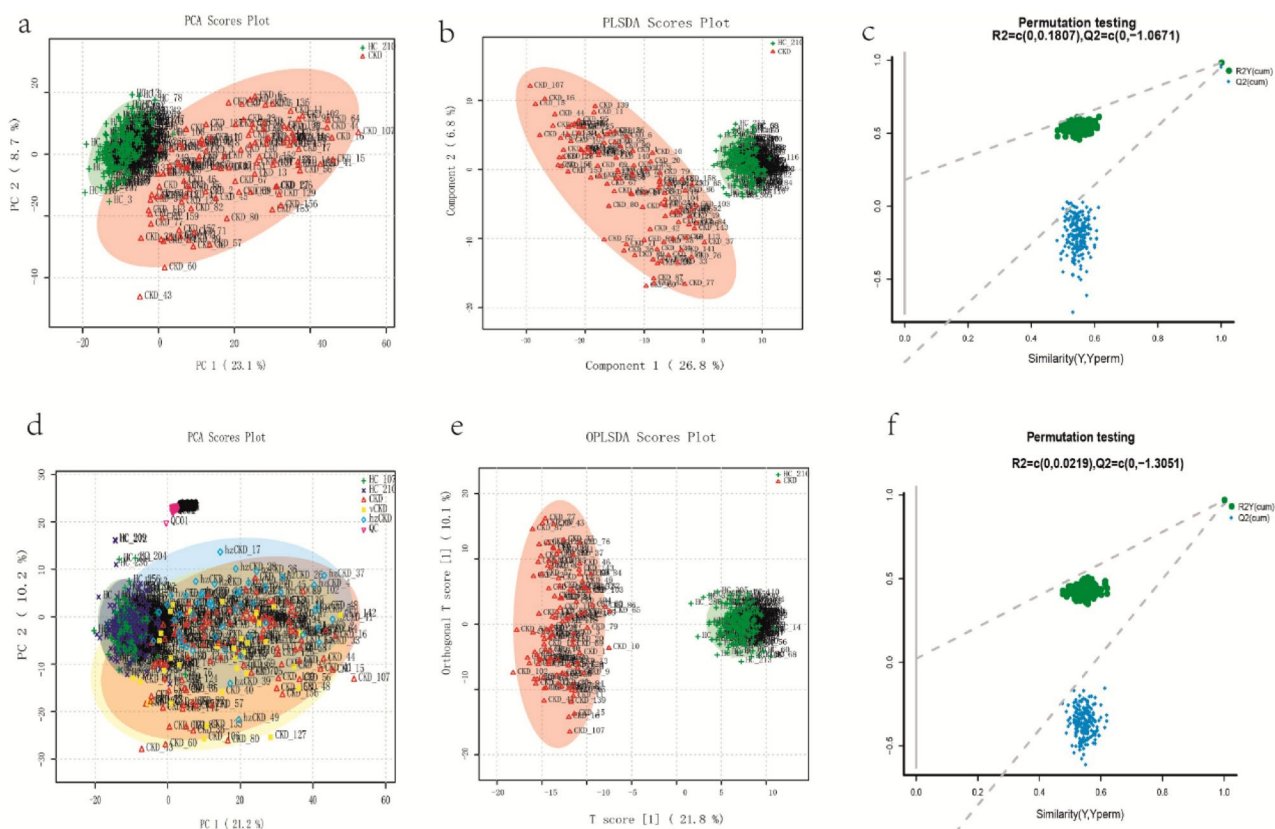


Figure 2. PCA (a), PLS-DA (b, c), and OPLS-DA (e, f) analysis score plots illustrate the metabolic of CKD and healthy controls. (d) QC samples (purple ∇) are intensively distributed. PLS-DA and OPLS-DA analysis score plots for metabolic profiles of CKD (red Δ) and HC (green $+$) show clear discrimination between the two groups. (c, f) Permutation testing was used to assess the reliability of the models. CKD: chronic kidney disease; HC: healthy control; PCA: principal component analysis; PLS-DA: Partial least squares discrimination analysis; OPLS-DA: orthogonal partial least squares discriminate analysis; QC: quality control.

and Online Supplementary Data S2). The volcano chart presents the relative expression of the identified metabolites in CKD compared with HC. Of these, 179 metabolites were upregulated, and 135 were downregulated (Figure 3 and Online Supplementary Data S2). Hence, the results indicate that the metabolomes of CKD and HC are different.

Metabolic pathway analysis

In order to understand the metabolic pathways and functions of the above-mentioned differential metabolites, KEGG ID numbers were obtained for all the metabolites from the relevant databases. A total of 52 metabolites and 56 metabolic pathways were queried (Online Supplementary Data S3–S4 and Figure S2). In BRITE A, the metabolites annotated for environmental information processing were inosine, melibiose, and L-glutamine, for human diseases, were L-glutamine, LysoPC(22:2(13Z,16Z)), and nicotine, for organismal systems were bilirubin, L-glutamine, and 14,15-DiHETrE. Fifty-two metabolites were annotated to metabolism, including L-glutamine, pyrrole-2-carboxylic acid, and N-formylmethionine. BRITE B included 21 branches and 37 metabolites annotated to global and overview maps, including N2-acetyl-L-ornithine, L-glutamine, and Hippuric acid. Fifteen metabolites were annotated to amino acid metabolism, including L-glutamine,

pyrrole-2-carboxylic acid, N2-acetyl-L-ornithine, and N-formylmethionine. Eight metabolites were annotated to 14,15-DiHETrE, nervonic acid, 9-OxoODE, and 9,10,13-TriHOME. (Figure S2 and Online Supplementary Data S5).

The six pathways that contained the highest number of differential metabolites were purine metabolism, caffeine metabolism, tyrosine metabolism, phenylalanine metabolism, ABC (ATP-binding cassette) transporters, and amino acid biosynthesis (Figure S3). There were four metabolites in the purine metabolism pathway (inosine, adenosine 3'-monophosphate, L-glutamine, and hypoxanthine), three metabolites in the caffeine metabolism pathway (1-methyluric acid, theophylline, and caffeine), and three metabolites in the tyrosine metabolism pathway (homovanillin, vanillylmandelic acid, and atrolactic acid) (Figure 4(a)).

The Metabolomics Pathway Analysis (MetPA) and the KEGG online database were used to explore the most relevant metabolic pathways and functions and reveal the underlying mechanisms of CKD at the metabolic level. As shown in Figure 4(b), 26 metabolic pathways were affected overall. The impact-value threshold calculated from the pathway topology analysis was set at 0.10. The top five pathways in plasma identified by P-value included (1) one carbon pool by folate, (2) pentose and glucuronate interconversions, (3) porphyrin and chlorophyll metabolism, (4) alanine, aspartate, and

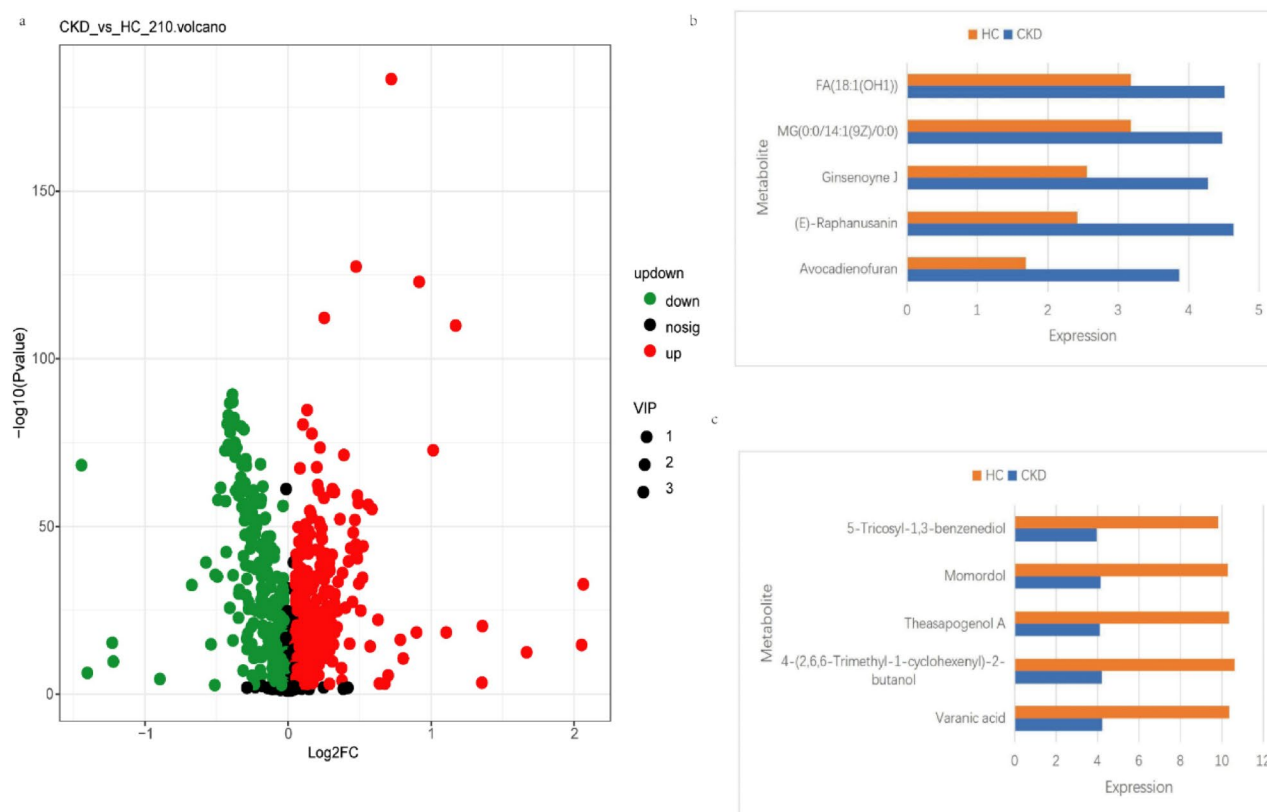


Figure 3. (a) Volcano diagrams showing the changes in CKD and healthy controls. The red dot on the right side of the figure represents the upregulated metabolite and the green dot on the left represents the downregulated metabolite. The x-axis corresponds to log2 (fold change), and the y-axis corresponds to $-\log_{10}$ (p-value). (b, c) the five metabolites with the most significant differences in expression. CKD: chronic kidney disease; HC: healthy control; VIP: variable importance in the projection; FC: fold change.

glutamate metabolism, and (5) folate biosynthesis (impact value >0.1) (Figure 4(b) and Online Supplementary Data S6).

The KEGG pathway enrichment analysis of the differential metabolites from CKD and HC was performed using Fisher's exact test. The results showed significant differences in important pathways, including caffeine metabolism, D-glutamine, and D-glutamate metabolism, purine metabolism, arginine biosynthesis, phenylalanine metabolism, and linoleic acid metabolism, with P-values of 0.0023, 0.0105, 0.0240, 0.0302, 0.0321, and 0.0425, respectively (Figure 4(c) and Online Supplementary Data S7). iPath 3.0 (interactive Pathways Explorer, <http://pathways.embl.de>) was used to visualize the metabolic pathways in the entire biological system (Figure S4).

Diagnostic potential for CKD based on serum metabolomics

In the training set, a random forest classifier model between 110 CKD and 210 HC was constructed to evaluate the potential of biomarkers in diagnosing CKD. Through the five-fold cross-validation of the random forest model, ten metabolites were selected as the best markers for CKD, including 9,10,13-TriHOME, (E)-raphanusanin, 9-OxoODE, and MG(0:0/14:1(9Z)/0:0). The probability of disease (POD) index for the training set, validation set, and cross-validation set was calculated using these ten best metabolites identified. In the

training set, compared with the HC group, the POD value of CKD was significantly higher, with an area under the curve (AUC) of 1 (95% confidence interval (CI): 0.9998-1). The data showed that the classifier model based on the serum differential metabolites could effectively distinguish CKD from HC.

Furthermore, 107 HC samples from Zhengzhou, 35 CKD samples from Zhengzhou, and 49 CKD samples from Hangzhou were combined to form a validation set and a cross-validation set to verify the effectiveness of the serum metabolomics classifier model for CKD. The data showed that the POD value of CKD in the two sets was significantly higher than for HC. In the validation set, the AUC of the POD index was 1 (95% CI: 1-1). In addition, in the cross-validation set, the POD index between CKD and HC reached an AUC of 0.9435 (95% CI: 0.8992-0.9879, $p < 0.0001$). These data confirmed the diagnostic potential of serum metabolomics for CKD (Figure 5). Serum metabolites can be used as a new diagnostic tool for CKD, but further research is needed for validation.

Metabolite correlation analysis and classification

Pearson's correlation analysis was used to analyze the correlation between pairs of metabolites (Figure S5 and Online Supplementary Data S8). The metabolites were classified based on their structure and function into nine categories (Figure S6).

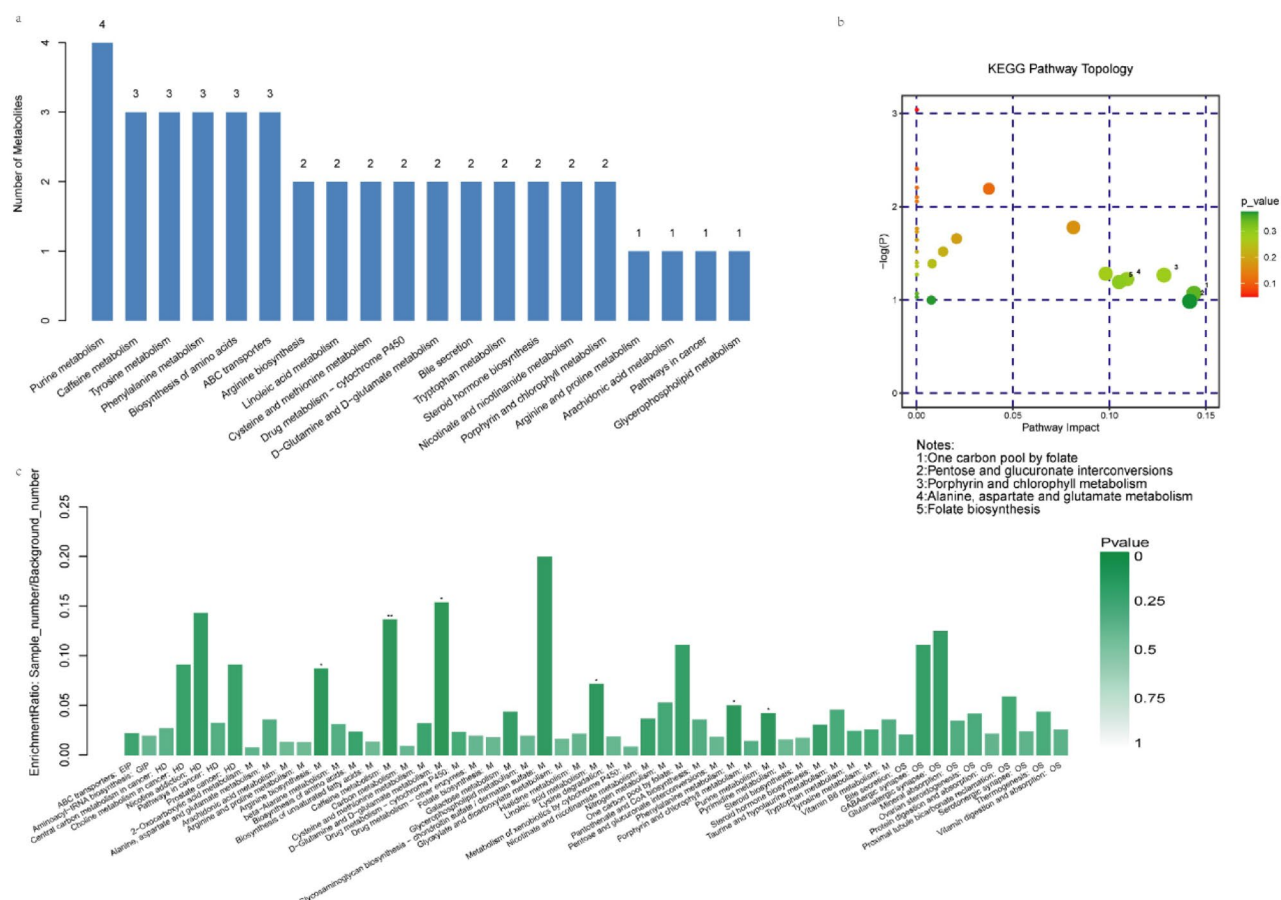


Figure 4. Results of pathways analysis of differential metabolites. (a) Contains statistics of the top 20 pathways with the most different metabolites. (b) Each bubble represents a KEGG pathway, the horizontal axis represents the relative importance of the metabolites in the pathway and the impact value; the vertical axis represents the significance of the enrichment of metabolites involved in the pathway $-\log_2(P)$ value. The size of the bubble is expressed by the representation of impact value. The color represents the p-value of pathway enrichment. Pathways were considered significantly enriched if the impact value >0.1 . (c) KEGG pathways enrichment analysis. Each column represents a pathway, and the height of the column represents the enrichment rate. The calculation formula is as follows: (enrichment ratio = sample number/background number). The color indicates the significance of the enrichment (P value). $p < 0.001$ is marked as ***, $p < 0.01$ is marked as **, and $p < 0.05$ is marked as *. KEGG: Kyoto Encyclopedia of Genes and Genomes.

Blood urea nitrogen (BUN) had a positive correlation with avocadienofuran, portulacaxanthin III, roxithromycin, repaglinide aromatic amine, and 11- β -Hydroxyandrosterone-3-glucuronide, while it had a negative correlation with myricanene B 5-[arabinosyl-(1 \rightarrow 6)-glucoside]. Uric acid (UA) was positively correlated with avocadienofuran, portulacaxanthin III, repaglinide aromatic amine, and 11- β -hydroxyandrosterone-3-glucuronide. Albumin (ALB) was positively correlated with myricanene B 5-[arabinosyl-(1 \rightarrow 6)-glucoside] and negatively correlated with avocadienofuran, portulacaxanthin III, roxithromycin, and repaglinide aromatic amine (Figure 6 and Online Supplementary Data S9).

Metabolomics analysis of different CKD stages

These were 39 CKD stage 1-2 samples (group A), 45 CKD stage 3-4 samples (group B), and 61 CKD stage 5 samples (group C). Then, 326 metabolites showed differences among the three groups (at the same time meeting $VIP > 1$, $p < 0.05$) (Online Supplementary Data S10). Based on KEGG, 52 metabolites, and 56 metabolic pathways were queried (Online

Supplementary Data S11-12). The four pathways that contained the highest number of differential metabolites were ABC transporters, phenylalanine metabolism, tyrosine metabolism, and amino acid biosynthesis. There were six metabolites in the ABC transporters pathway (myo-inositol, L-glutamine, and melibiose). Phenylacetylglycine, hippuric acid, and benzoic acid were in the phenylalanine metabolism pathway (Online Supplementary Data S13). MetPA analysis indicated that these biomarkers closely correlated with various metabolic pathways involved in CKD pathogenesis, including the arginine biosynthesis pathway, biotin metabolism, inositol phosphate metabolism, and alanine, aspartate, and glutamate metabolism (Online Supplementary Data S14). KEGG enrichment analysis showed that 52 pathways were enriched, out of which six signaling pathways were significantly enriched ($p < 0.05$), including arginine biosynthesis pathway, caffeine metabolism, phenylalanine metabolism, galactose metabolism, and ABC transporters (Online Supplementary Data S15). Metabolite classification showed that 14 metabolites could be divided into 11 categories (Online Supplementary Data S16).

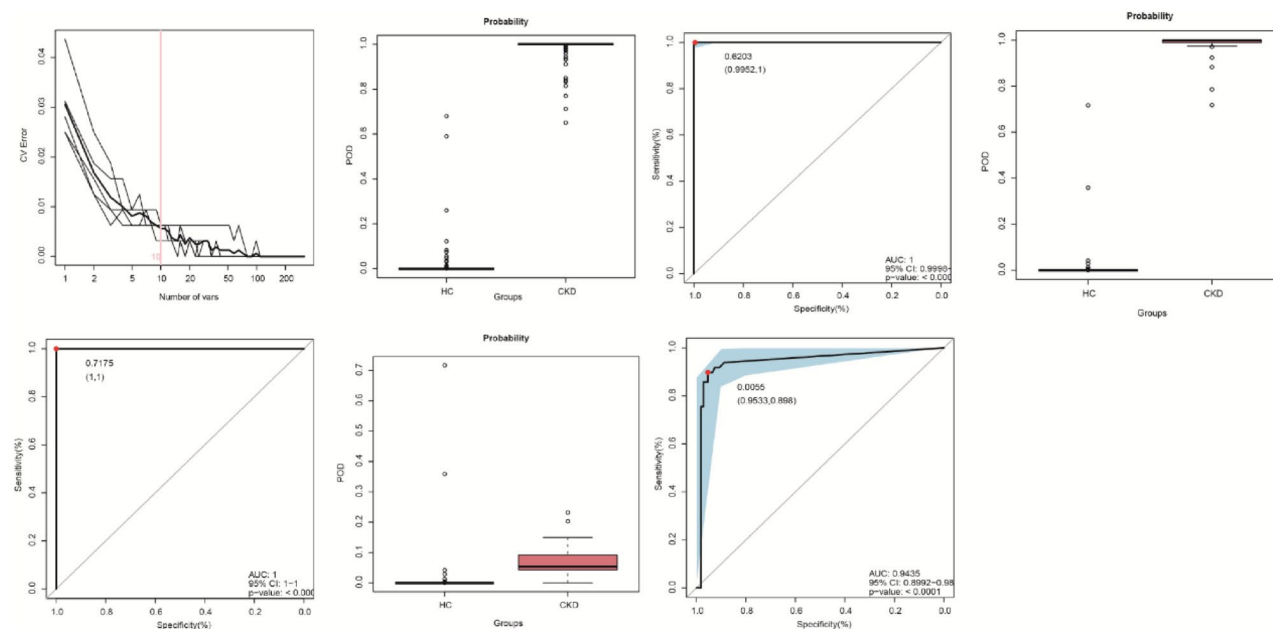


Figure 5. The diagnostic potential of serum metabolomics in CKD. (a) Ten serum biomarkers were selected as the optimal markers set by the random Forest model. (b) The POD value was significantly increased in CKD ($n=110$) versus HC ($n=210$) in the training set. (c) The POD index achieved an AUC value of 1 with a 95% CI of 0.9998 to 1 between CKD ($n=110$) versus HC ($n=210$) in the training set. The POD value was significantly increased in CKD compared with HCs and achieved good diagnostic efficacy in the validation set (d, e) and cross-validation set (f, g). CKD: chronic kidney disease; HC: healthy control; AUC: the area under the curve; CI: confidence interval; POD: the probability of disease.

The differences between serum metabolic profiles at different clinical stages of the disease were examined. With the progression of CKD, the levels of seven metabolites (including 2-hydroxyestrone-1-S-glutathione, 16-bromo-9E-hexadecenoic acid, and 3,8-dihydroxy-6-methoxy-7(11)-eremophilene-12,8-olide), gradually decreased, while the levels of 190 other metabolites (including nicotine, 3-hydroxycarbamazepine, 2-indolecarboxylic acid, and 2-carboxy-4-dodecanolide) gradually increased (Figure 7).

Fourteen clinical indicators (UA, eGFR, erythrocyte sedimentation rate, hypertension, total cholesterol, potassium, red blood cells (RBC), stage, low-density lipoprotein, point urine protein, phosphorus, triglycerides, complement 3, and procalcitonin) were closely related to the identified metabolites. eGFR negatively correlated with salicyluric β -D-glucuronide and 8-acetylegelolide. The stage of disease positively correlated with three metabolites in particular (trans-resveratrol 3,4'-disulfate, salicyluric β -D-glucuronide, and 8-acetylegelolide). RBC was found to negatively correlate with 12 metabolites (including cyclocalopin C1, scytalone, 11- β -hydroxyandrosterone-3-glucuronide, and 2-carboxy-4-dodecanolide). Furthermore, 11- β -hydroxyandrosterone-3-glucuronide and ent-6R-16bOH-17-trihydroxy-7-oxo-6-7-seco-19-6-kauranolide-6-O-glucoside were positively correlated with the operational taxonomic unit 19 (OTU19) (*Akkermansia*). 11- β -hydroxyandrosterone-3-glucuronide, trans-resveratrol-3-4-disulfate, and ent-6R-16bOH-17-trihydroxy-7-oxo-6-7-seco-19-6-kauranolide-6-O-glucoside positively correlated with OTU225 (*Bacteroides*). Cyclocalopin-C1 and 11- β -hydroxyandrosterone-3-glucuronide were negatively correlated with OTU161 (*Veillonella*) (Figure 6b and Online Supplementary Data S17).

Finally, random forest classifier models were constructed to differentiate between CKD-A and CKD-B, CKD-A and CKD-C, and CKD-B and CKD-C. Indole-3-carboxylic acid and (3-arylcarbonyl)-alanine were selected as the optimal marker set between CKD-A and CKD-B. The POD index achieved an AUC value of 0.9595 (95% CI: 0.8990-1) for CKD-A vs. CKD-B ($p < 0.0001$). Semilepidinoside B, uridine, N-(1-deoxy-1-fructosyl)-valine, and nepsilon-acetyl-L-lysine were selected as the optimal marker set between CKD-A and CKD-C. The POD index achieved an AUC value of 1 (95% CI: 1-1) for CKD-A vs. CKD-C ($p < 0.0001$). Asarylaldehyde, hydantoin-5-propionic acid, 1-methylinosine, and N6-acetyl-LL-2,6-diaminoheptanedioate were selected as the optimal marker set between CKD-B and CKD-C. The POD index achieved an AUC value of 0.9273 (95% CI: 0.8564-0.9982) for CKD-B vs. CKD-C ($p < 0.01$). These results indicate that these metabolites could be biomarkers for CKD staging.

Discussion

CKD is one of the most concerning public health issues worldwide. The early detection of kidney disease, careful monitoring of kidney function, and timely response to treatment interventions are essential for the timely diagnosis and prevention of the progression and complications of CKD. The present study comprehensively clarified the serum metabolomics characteristics of patients with CKD using a large study sample from China. Functional and classification analyses of the differential metabolites were performed, and the correlations between metabolites, the intestinal microbiota, and clinical indicators were examined. A CKD diagnostic model

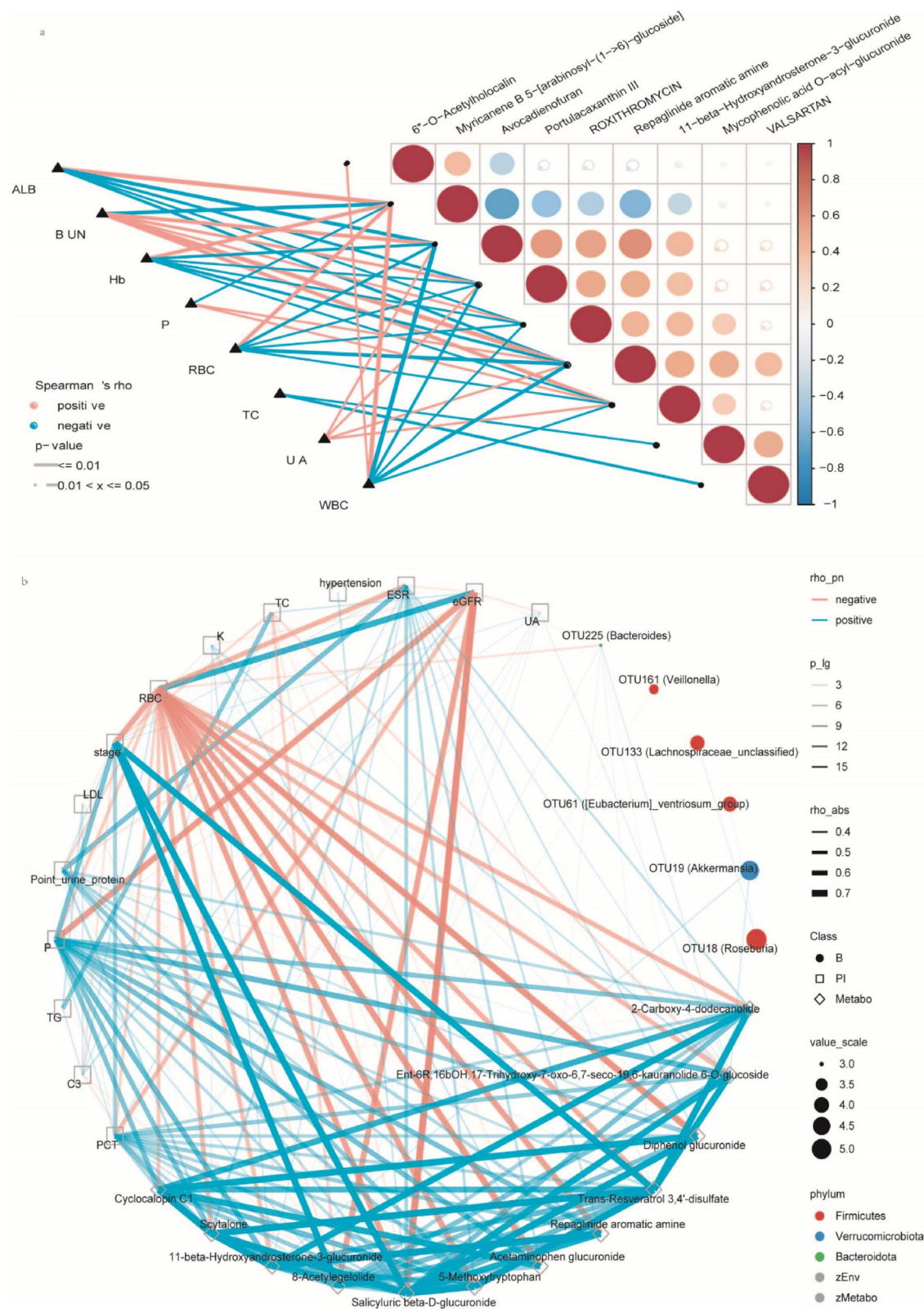


Figure 6. (a) Spearman correlation coefficient showing the partial spearman's correlation coefficients among nine metabolites and eight clinical indicators of CKD ($n=110$). The blue line indicates a positive correlation, while red indicates a negative. The thickness of the line represents the size of the correlation coefficient. (b) Spearman correlation coefficient shows the partial spearman's correlation coefficients among 12 metabolites, 6 OTUs, and 14 clinical indicators of CKD ($n=145$). □ indicates clinical indicators. ◇ indicates metabolites. ● indicates OTUs. The thickness of the line represents the size of the correlation coefficient. CKD: chronic kidney disease; OTU: operational taxonomic unit.

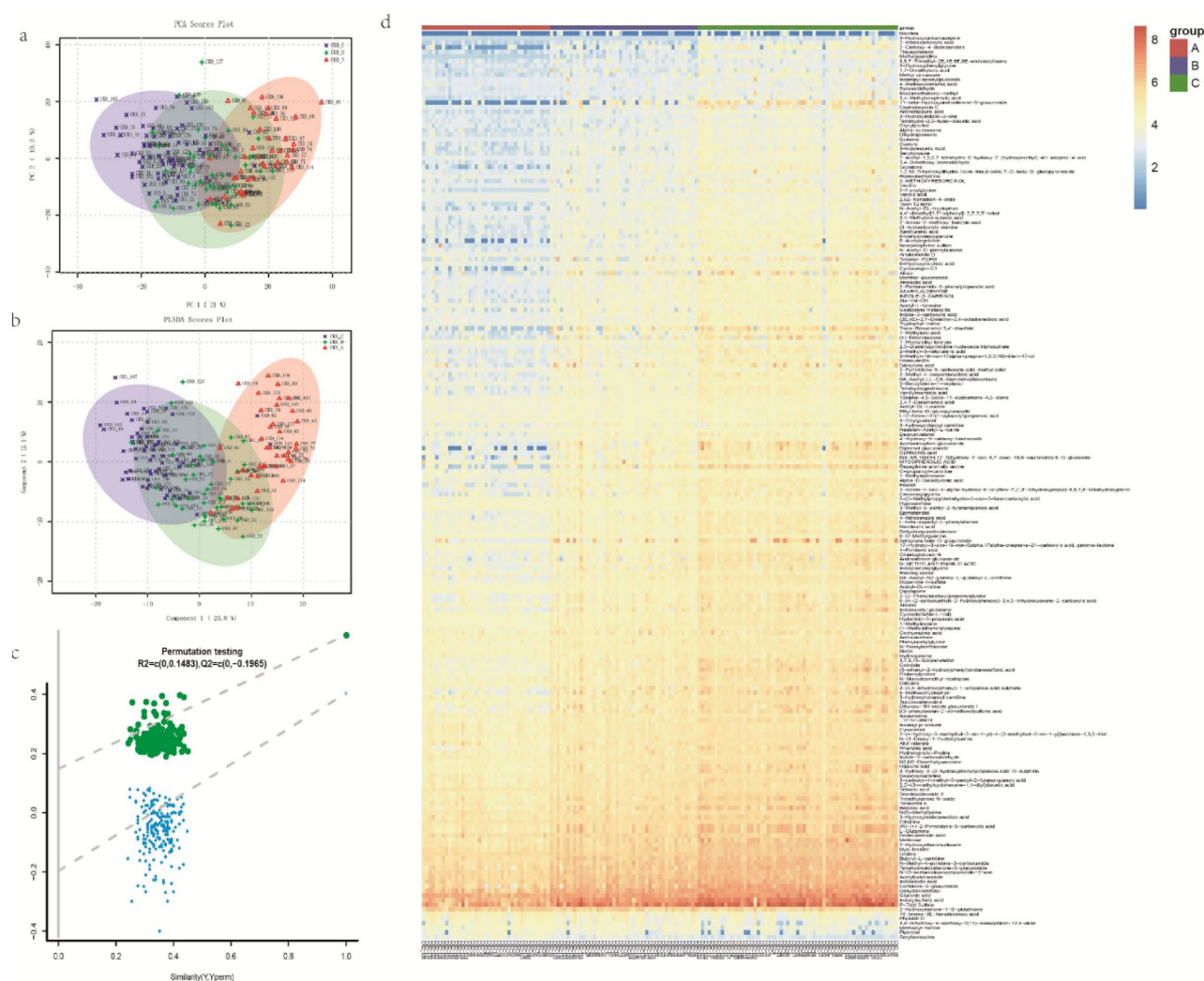


Figure 7. PCA (a) and PLS-DA (b, c) analysis score plots illustrate the metabolomic of CKD-A, CKD-B, and CKD-C. PCA and PLS-DA analysis score plots for metabolic profiles of CKD-A (red Δ), CKD-B (green +), and CKD-C (blue \times), showing clear discrimination between the three groups. (c) Permutation testing was used to assess the reliability of the models. (d) Each column represents a sample. From left to right are CKD-A, CKD-B, and CKD-C, and each row represents a metabolite. The color in the figure represents the relative expression level of the metabolite in the group of samples. The specific expression changes are shown in the numbers beside the color bar at the top right. CKD: chronic kidney disease; PCA: principal component analysis; PLS-DA: partial least squares discrimination analysis; CKD-A, group A of CKD; CKD-B, group B of CKD; CKD-C, group C of CKD.

was also successfully established, and the model achieved external validation.

The present study showed that the serum metabolomics of patients with CKD was significantly different from that of healthy controls. A total of 314 metabolites with significant differences were identified and were related to multiple metabolic pathways and disorders. Using relevant databases, 52 highly relevant metabolites were found, participating in 56 metabolic pathways. The CKD serum metabolomics differences were reflected in various biological pathways such as caffeine metabolism, arginine biosynthesis, purine metabolism, D-glutamine, and D-glutamate metabolism. A previous study highlighted several metabolites that could be used for kidney diseases [12]. Xu et al. [15] identified several lipids and could be used as biomarkers for diabetic nephropathy. Still, the metabolomics approach is subjected to the analytical method used to examine the metabolites, and different studies that used different analytic methods should not be directly compared.

Among the identified metabolites, many have been confirmed to be involved in the development of CKD. Oxidative stress and inflammation are important features of CKD and its complications (such as cardiovascular disease, hypertension, and anemia), as well as the main mediators of its occurrence and progression [18, 19]. Some of the metabolites have been confirmed to be uremic toxins, and many of them are believed to play a role in the progression of CKD and cardiovascular diseases (CVD), such as indoxyl sulfate (IS) [20], 3-methylamine oxide (TMAO) [21], p-cresyl sulfate (PCS) [22], indole-3-acetic acid (IAA) [23], and hippuric acid. CVD is the leading cause of morbidity and mortality in patients with CKD or end-stage renal disease. PCS, IS, and IAA have been confirmed to induce endothelial dysfunction, oxidative stress, activation of signaling pathways (e.g. aromatic hydrocarbon receptor (AhR), nuclear factor kappa B (NF- κ B), and mitogen-activated protein kinase (MAPK) pathways), and the formation of endothelial microparticles that further promote

the occurrence of CVD [24]. PCS can also contribute to kidney injury and fibrosis by inducing epithelial-to-mesenchymal transition and the expression of inflammatory factors [25]. IS accumulates in CKD and can lead to pathological fibrosis, thereby promoting the development and progression of CKD [26,27]. A study demonstrated that hippuric acid could increase oxidative stress by decreasing the expression of Nrf2 (nuclear factor erythroid 2 related factors) and its downstream antioxidant enzymes to promote the progression of renal fibrosis [28–33]. Hence, multiple metabolites can induce the development of CKD through oxidative stress and chronic inflammation, while 5-methoxytryptophan (5-MTP) and rhein can effectively control the inflammatory response, reduce tissue damage, and reduce fibrosis. 5-MTP is a relatively new endothelial factor with vascular protection and anti-inflammatory effects [34, 35]. In the development of CKD, the reduction of tryptophan raw materials and the destruction of endothelial cells by LPS and inflammatory mediators can all lead to the reduction of 5-MTP production [36, 37]. Rhein can inhibit kidney inflammation by reducing the level of reactive oxygen species and inhibiting oxidative stress pathways, thereby protecting the kidneys [38]. Therefore, the weakened anti-inflammatory effect could lead to the decline of the kidney's ability to resist oxidative stress and fibrosis, which leads to the occurrence of CKD.

At the same time, serum metabolites can serve as potential therapeutic targets for CKD. 5-MTP can potentially be a drug for treating kidney diseases caused by ischemia-reperfusion injury [39]. IS can effectively induce the expression of cytochrome P450 family 1 subfamily B member 1 (CYP1B1) via the AHR pathway, and *in vitro* and *in vivo* studies have shown that CYP1B1 knockdown or inhibition with 2,4,3',5'-tetra methoxy stilbene (TMS) may reverse cardiac hypertrophy induced by IS, which may be a potential therapeutic target for CVD among patients with CKD [40]. Kelch-like ECH-associated protein 1 (Keap1) is the main Nrf2 repressor protein. The small molecule Nrf2 activator bardoxolone methyl targeting Keap1 is beneficial in all kidney diseases [39]. Keap1-Nrf2 protein-protein interaction inhibitor CPUY192002, pyrrolidine dithiocarbamate, and Celastrol can effectively inhibit the chronic inflammation of CKD [41, 42]. Iodomethylcholine (IMC) can significantly reduce multiple markers of renal injury (plasma creatinine, cystatin C, and TMAO) and attenuate the development of CKD and cardiac hypertrophy [21]. Hyperphosphatemia is a central risk factor of CKD-associated mineral and bone disorder (CKD-MBD), which is one of the complications during CKD and usually leads to CVD. Niacin and its compounds can reduce serum phosphate levels by inhibiting intestinal phosphate transport [43, 44]. Hence, metabolites can improve kidney damage and fibrosis by inhibiting chronic inflammation and oxidative stress and reducing metabolite levels. Nevertheless, clinical trials are needed to determine their effectiveness, safety, and tolerability.

The random forest model identified 10 optimal metabolic markers that can be used to distinguish patients with CKD from healthy individuals. Among them, bilirubin has been confirmed to reduce oxidative stress and improve renal

tubular damage and interstitial fibrosis. The serum bilirubin levels in patients with CKD are significantly lower than in healthy people [45]. It is worth noting that the present study also identified metabolites that can be used to stage CKD. Indeed, the serum levels of seven metabolites were found to decrease with the progress of CKD, while the levels of four accumulated with disease progression. Among them, methyl guanidine and myo-inositol showed a significant positive correlation with creatinine [46, 47], TMAO showed a negative correlation with eGFR [3], and the levels of indole-3-acetic acid (IAA) were found to be much higher in the more advanced stages of CKD [23]. Of note, the prediction models for CKD and CKD staging all had AUCs >0.95, indicating a very high predictive value for CKD and CKD staging. These performances are higher than the model by Xu et al. [15] (based only on lipid metabolites) that showed an AUC of 0.77 and 66% sensitivity, and 77% specificity. Still, additional studies are necessary for model validation.

The gut microbiota is important in health and disease [48, 49]. The gut microbiome can be used to diagnose CKD early [50]. Multiple studies showed that the gut microbiome affects the blood metabolome in CKD cases [51, 52], and some uremic toxins have been derived from the intestinal microbial metabolism of dietary amino acids. Tryptophan is an essential aromatic amino acid, considered important among many metabolites in the crosstalk between gut microbiota and the host [53, 54]. The host and gut microbiota produce large amounts of uremic toxins derived from tryptophan metabolism, which are associated with renal fibrosis. For example, *Lactobacillus*, *Bacteroides*, *Bifidobacterium*, *Peptostreptococcus*, *Rumenococcus*, *Clostridium rumen*, and *Clostridium* can metabolize tryptophan into indole and indole derivatives, such as tryptamine, IAA, and indole-3-propionic acid (IPA) [55, 56]. *Peptostreptococcus spp* can convert tryptophan into IPA in the gut [55]. Tryptophan is metabolized by bacterial tryptophan enzymes to produce the precursor indoles, and the latter can be converted to IS [57]. Tryptophan metabolites accumulate in the blood and participate in renal fibrosis [58]. The aromatic amino acid tyrosine is transformed into phenol, p-cresol, and other phenolic compounds through the fermentation of bacteria such as *Bacteroides*, *Bifidobacterium*, *Clostridium*, *Enterobacteriaceae*, and *Enterococcus*. P-cresol can be converted into PCS, and the latter can promote the progress of CKD [25]. Probiotics and AST-120 (an oral spherical activated carbon) can reduce the production of uremic toxins by regulating intestinal microecology and adsorbing the precursors of PCS in the intestine, respectively, thereby delaying the progress of CKD [59, 60]. Sonnenburg et al. used antibiotics in combination with the recolonization of tryptophanase-deficient strains to reduce the amount of indole produced in the intestine, thereby reducing the levels of circulating IS [61]. Studies have found that isoquercitrin (ISO) can inhibit the production of indole mediated by the gut microbiota to reduce the IS concentration and delay the progression of CKD [62]. Therefore, delaying or curing diseases by regulating the intestinal microbiota can become an important breakthrough.

This study had limitations. Only one analysis method was used, which can limit the variety and number of identified metabolites. Second, no HCs were enrolled from Hangzhou, and these patients could only serve for external validation. Considering the large number of patients with CKD, the sample size was small, and the results must be validated in larger studies. Finally, only serum metabolomics was analyzed. Future studies should also examine urinary and fecal metabolomics.

In conclusion, this study identified serum metabolomic characteristics of patients with CKD. The characteristics of serum metabolism at different CKD clinical stages were analyzed. Nevertheless, the analysis of serum metabolomics provides reliable information that lays the ground for further research on the occurrence and progression of CKD.

Acknowledgements

The authors thank all the clinical doctors who were involved in this study. The authors also thank the generous volunteers who enrolled in the study.

Authors' contributions

Conceptualization, G.W. and Z.L.; Methodology, X.G., Y.D., G.W. and Z.L.; Software, H.R., and C.L.; Validation, G.L., Y.H., H.R., and C.L.; Formal Analysis, X.W., Z.R., H.R., and C.L.; Investigation, X.G., Y.D., X.W., Z.R., S.D. and W.L.; Resources, X.G., Y.D., S.G., Y.F., S.D. and W.L.; Data Curation, J.W., S.G. and Y.F.; Writing – Original Draft Preparation, X.G., Y.D., and G.W.; Writing – Review & Editing, X.G., Y.D., G.W. and Z.L.; Visualization, X.G., Y.D., G.W. and Z.L.; Supervision, G.W. and Z.L.; Project Administration, G.W. and Z.L.; Funding Acquisition, Z.R., G.W. and Z.L.

Ethics approval and consent to participate

The study was carried out in accordance with the Declaration of Helsinki. The study was reviewed and approved by the Institutional Review Board of the First Affiliated Hospital of Zhengzhou University (# 2021-KY-0655). All participants signed written informed consent after the study protocol was fully explained.

Consent for publication

Not applicable.

Disclosure statement

No potential conflict of interest was reported by the author(s).

Funding

The study was supported by the Henan Provincial Medical Science and Technology Project (SBGJ2018035), the Key Projects of Henan Province Colleges and Universities

(21A320060), Henan Province Science and Technology Innovation Personnel Training Project (YXKC2022018), the National Key Research and Development Program of China (2018YFC2000500), and the National Natural Science Foundation of China (U2004121).

ORCID

Ge Wu  <http://orcid.org/0000-0003-1941-7722>

Data availability statement

All data generated or analyzed during this study are included in this published article.

References

Uncategorized References

- [1] Webster AC, Nagler EV, Morton RL, et al. Chronic kidney disease[J]. *The Lancet*. 2017;389(10075):1238–1252. doi: [10.1016/S0140-6736\(16\)32064-5](https://doi.org/10.1016/S0140-6736(16)32064-5).
- [2] Global, regional, and national burden of chronic kidney disease, 1990–2017: a systematic analysis for the Global Burden of Disease Study 2017. *Lancet* (London, England). 2020;395(10225):709–733. doi: [10.1016/S0140-6736\(20\)30045-3](https://doi.org/10.1016/S0140-6736(20)30045-3).
- [3] Guo F, Dai Q, Zeng X, et al. Renal function is associated with plasma trimethylamine-N-oxide, choline, L-carnitine and betaine: a pilot study. *Int Urol Nephrol*. 2021;53(3):539–551. doi: [10.1007/s11255-020-02632-6](https://doi.org/10.1007/s11255-020-02632-6).
- [4] Romagnani P, Remuzzi G, Glasscock R, et al. Chronic kidney disease. *Nat Rev Dis Primers*. 2017;3(1):17088. doi: [10.1038/nrdp.2017.88](https://doi.org/10.1038/nrdp.2017.88).
- [5] Wang Y, Ma S, Chen Y, et al. Chronic kidney disease: biomarker diagnosis to therapeutic targets. *Clin Chim Acta*. 2019;499:54–63. doi: [10.1016/j.cca.2019.08.030](https://doi.org/10.1016/j.cca.2019.08.030).
- [6] Zhang Z, Chen H, Vaziri N, et al. Metabolomic signatures of chronic kidney disease of diverse etiologies in the rats and humans. *J Proteome Res*. 2016;15(10):3802–3812. doi: [10.1021/acs.jproteome.6b00583](https://doi.org/10.1021/acs.jproteome.6b00583).
- [7] Lousa I, Reis F, Beirão I, et al. New potential biomarkers for chronic kidney disease management—a review of the literature. *Int J Mol Sci*. 2020;22(1):22. doi: [10.3390/ijms22010043](https://doi.org/10.3390/ijms22010043).
- [8] Yan Z, Wang G, Shi X. Advances in the progression and prognosis biomarkers of chronic kidney disease. *Front Pharmacol*. 2021;12:785375. doi: [10.3389/fphar.2021.785375](https://doi.org/10.3389/fphar.2021.785375).
- [9] Higashisaka K, Takeya S, Kamada H, et al. Identification of biomarkers of chronic kidney disease among kidney-derived proteins. *Clin Proteomics*. 2022;19(1):3. J doi: [10.1186/s12014-021-09340-y](https://doi.org/10.1186/s12014-021-09340-y).
- [10] Chen D, Chen H, Chen L, et al. The link between phenotype and fatty acid metabolism in advanced chronic kidney disease. *Nephrol Dial Transplant*. 2017;32(7):1154–1166. J doi: [10.1093/ndt/gfw415](https://doi.org/10.1093/ndt/gfw415).
- [11] Levin A, Tonelli M, Bonventre J, et al. Global kidney health 2017 and beyond: a roadmap for closing gaps in care, research, and policy. *Lancet*. 2017;390(10105):1888–1917. doi: [10.1016/S0140-6736\(17\)30788-2](https://doi.org/10.1016/S0140-6736(17)30788-2).

- [12] Weiss R, Kim K. Metabolomics in the study of kidney diseases. *Nat Rev Nephrol*. 2011;8(1):22–33. doi: [10.1038/nrneph.2011.152](https://doi.org/10.1038/nrneph.2011.152).
- [13] Bartenbach L, Karall T, Koch J, et al. Amino acid and phospholipid metabolism as an indicator of inflammation and subtle cardiomyopathy in patients with Marfan syndrome[J]. *Metabolites*. 2021;11(12):805. doi: [10.3390/metabo11120805](https://doi.org/10.3390/metabo11120805).
- [14] Fort PE, Rajendiran TM, Soni T, et al. Diminished retinal complex lipid synthesis and impaired fatty acid beta-oxidation associated with human diabetic retinopathy. *JCI Insight*. 2021;6(19):e152109. doi: [10.1172/jci.insight.152109](https://doi.org/10.1172/jci.insight.152109).
- [15] Xu T, Xu X, Zhang L, et al. Lipidomics reveals serum specific lipid alterations in diabetic nephropathy. *Front Endocrinol (Lausanne)*. 2021;12:781417. doi: [10.3389/fendo.2021.781417](https://doi.org/10.3389/fendo.2021.781417).
- [16] Kidney Disease: improving Global Outcomes Diabetes Work G. KDIGO 2020 Clinical Practice Guideline for Diabetes Management in Chronic Kidney Disease. *Kidney Int*. 2020;98(4S):S1–S115.
- [17] Acharjee A, Larkman J, Xu Y, et al. A random forest based biomarker discovery and power analysis framework for diagnostics research. *BMC Med Genomics*. 2020;13(1):178. doi: [10.1186/s12920-020-00826-6](https://doi.org/10.1186/s12920-020-00826-6).
- [18] Himmelfarb J, Hakim R. Oxidative stress in uremia. *Curr Opin Nephrol Hypertens*. 2003;12(6):593–598. doi: [10.1097/00041552-200311000-00004](https://doi.org/10.1097/00041552-200311000-00004).
- [19] Vaziri N. Oxidative stress in uremia: nature, mechanisms, and potential consequences. *Semin Nephrol*. 2004;24(5):469–473. doi: [10.1016/j.semnephrol.2004.06.026](https://doi.org/10.1016/j.semnephrol.2004.06.026).
- [20] Gao H, Liu S. Role of uremic toxin indoxyl sulfate in the progression of cardiovascular disease. *Life Sci*. 2017;185:23–29. doi: [10.1016/j.lfs.2017.07.027](https://doi.org/10.1016/j.lfs.2017.07.027).
- [21] Zhang W, Miikeda A, Zuckerman J, et al. Inhibition of microbiota-dependent TMAO production attenuates chronic kidney disease in mice. *Sci Rep*. 2021;11(1):518. doi: [10.1038/s41598-020-80063-0](https://doi.org/10.1038/s41598-020-80063-0).
- [22] Lin C, Wu V, Wu P, et al. Meta-analysis of the associations of p-cresyl sulfate (PCS) and indoxyl sulfate (IS) with cardiovascular events and all-cause mortality in patients with chronic renal failure. *PLoS One*. 2015;10(7):e0132589. doi: [10.1371/journal.pone.0132589](https://doi.org/10.1371/journal.pone.0132589).
- [23] Dou L, Sallée M, Cerini C, et al. The cardiovascular effect of the uremic solute indole-3 acetic acid. *J Am Soc Nephrol*. 2015;26(4):876–887. doi: [10.1681/ASN.2013121283](https://doi.org/10.1681/ASN.2013121283).
- [24] Cunha R, Santos A, Barreto F, et al. How do uremic toxins affect the endothelium? *Toxins (Basel)*. 2020;12(6):412. doi: [10.3390/toxins12060412](https://doi.org/10.3390/toxins12060412).
- [25] Gryp T, Vanholder R, Vanechoutte M, et al. Cresyl sulfate. *Toxins (Basel)*. 2017;9(2):9. doi: [10.3390/toxins9020052](https://doi.org/10.3390/toxins9020052).
- [26] Tumor Z, Shimizu H, Enomoto A, et al. Indoxyl sulfate upregulates expression of ICAM-1 and MCP-1 by oxidative stress-induced NF-kappaB activation. *Am J Nephrol*. 2010;31(5):435–441. doi: [10.1159/000299798](https://doi.org/10.1159/000299798).
- [27] Shimizu H, Bolati D, Higashiyama Y, et al. Indoxyl sulfate upregulates renal expression of MCP-1 via production of ROS and activation of NF-kB, p53, ERK, and JNK in proximal tubular cells. *Life Sci*. 2012;90(13–14):525–530. doi: [10.1016/j.lfs.2012.01.013](https://doi.org/10.1016/j.lfs.2012.01.013).
- [28] Sun B, Wang X, Liu X, et al. Hippuric acid promotes renal fibrosis by disrupting redox homeostasis via facilitation of NRF2-KEAP1-CUL3 interactions in chronic kidney disease. *Antioxidants (Basel)*. 2020;9(9):783. doi: [10.3390/antiox9090783](https://doi.org/10.3390/antiox9090783).
- [29] Jiang T, Huang Z, Lin Y, et al. The protective role of Nrf2 in streptozotocin-induced diabetic nephropathy. *Diabetes*. 2010;59(4):850–860. doi: [10.2337/db09-1342](https://doi.org/10.2337/db09-1342).
- [30] Tsai P, Ka S, Chao T, et al. Antroquinonol reduces oxidative stress by enhancing the Nrf2 signaling pathway and inhibits inflammation and sclerosis in focal segmental glomerulosclerosis mice. *Free Radic Biol Med*. 2011;50(11):1503–1516. doi: [10.1016/j.freeradbiomed.2011.02.029](https://doi.org/10.1016/j.freeradbiomed.2011.02.029).
- [31] Yang S, Ka S, Hua K, et al. Antroquinonol mitigates an accelerated and progressive IgA nephropathy model in mice by activating the Nrf2 pathway and inhibiting T cells and NLRP3 inflammasome. *Free Radic Biol Med*. 2013;61:285–297. doi: [10.1016/j.freeradbiomed.2013.03.024](https://doi.org/10.1016/j.freeradbiomed.2013.03.024).
- [32] Kim H, Vaziri N. Contribution of impaired Nrf2-Keap1 pathway to oxidative stress and inflammation in chronic renal failure. *Am J Physiol Renal Physiol*. 2010;298(3):F662–71. doi: [10.1152/ajprenal.00421.2009](https://doi.org/10.1152/ajprenal.00421.2009).
- [33] Rinaldi Tosi M, Bocanegra V, Manucha W, et al. The Nrf2-Keap1 cellular defense pathway and heat shock protein 70 (Hsp70) response. Role in protection against oxidative stress in early neonatal unilateral ureteral obstruction (UUO). *Cell Stress Chaperones*. 2011;16(1):57–68. doi: [10.1007/s12192-010-0221-y](https://doi.org/10.1007/s12192-010-0221-y).
- [34] Wang Y, Hsu Y, Wu H, et al. Endothelium-derived 5-methoxytryptophan is a circulating anti-inflammatory molecule that blocks systemic inflammation. *Circ Res*. 2016;119(2):222–236. doi: [10.1161/CIRCRESAHA.116.308559](https://doi.org/10.1161/CIRCRESAHA.116.308559).
- [35] Cheng H, Kuo C, Yan J, et al. Control of cyclooxygenase-2 expression and tumorigenesis by endogenous 5-methoxytryptophan. *Proc Natl Acad Sci USA*. 2012;109(33):13231–13236. doi: [10.1073/pnas.1209919109](https://doi.org/10.1073/pnas.1209919109).
- [36] Suliman M, Qureshi A, Stenvinkel P, et al. Inflammation contributes to low plasma amino acid concentrations in patients with chronic kidney disease. *Am J Clin Nutr*. 2005;82(2):342–349. doi: [10.1093/ajcn.82.2.342](https://doi.org/10.1093/ajcn.82.2.342).
- [37] Wu K, Kuo C, Yet S, et al. 5-methoxytryptophan: an arsenal against vascular injury and inflammation. *J Biomed Sci*. 2020;27(1):79. doi: [10.1186/s12929-020-00671-w](https://doi.org/10.1186/s12929-020-00671-w).
- [38] Hu G, Liu J, Zhen Y, et al. Rhein lysinate increases the median survival time of SAMP10 mice: protective role in the kidney. *Acta Pharmacol Sin*. 2013;34(4):515–521. doi: [10.1038/aps.2012.177](https://doi.org/10.1038/aps.2012.177).
- [39] Wang W, Chang C, Sun M, et al. DPP-4 inhibitor attenuates toxic effects of indoxyl sulfate on kidney tubular cells. *PLoS One*. 2014;9(4):e93447. doi: [10.1371/journal.pone.0093447](https://doi.org/10.1371/journal.pone.0093447).
- [40] Zhang Y, Wang S, Huang Y, et al. Inhibition of CYP1B1 ameliorates cardiac hypertrophy induced by uremic toxin. *Mol Med Rep*. 2020;21(1):393–404. doi: [10.3892/mmr.2019.10810](https://doi.org/10.3892/mmr.2019.10810).
- [41] Lv W, Booz G, Wang Y, et al. Inflammation and renal fibrosis: recent developments on key signaling molecules as potential therapeutic targets. *Eur J Pharmacol*. 2018;820:65–76. doi: [10.1016/j.ejphar.2017.12.016](https://doi.org/10.1016/j.ejphar.2017.12.016).
- [42] Lu M, Zhao J, Liu Y, et al. CPUY192018, a potent inhibitor of the Keap1-Nrf2 protein-protein interaction, alleviates renal inflammation in mice by restricting oxidative stress and NF-kB activation. *Redox Biol*. 2019;26:101266. doi: [10.1016/j.redox.2019.101266](https://doi.org/10.1016/j.redox.2019.101266).

- [43] Ginsberg C, Ix J. Nicotinamide and phosphate homeostasis in chronic kidney disease. *Curr Opin Nephrol Hypertens*. 2016;25(4):285–291. doi: [10.1097/MNH.0000000000000236](https://doi.org/10.1097/MNH.0000000000000236).
- [44] Jin Kang H, Kim D, Mi Lee S, et al. Effects of low-dose niacin on dyslipidemia and serum phosphorus in patients with chronic kidney disease. *Kidney Res Clin Pract*. 2013;32(1):21–26. doi: [10.1016/j.krcp.2012.12.001](https://doi.org/10.1016/j.krcp.2012.12.001).
- [45] Li J, Liu D, Liu Z. Serum total bilirubin and progression of chronic kidney disease and mortality: a systematic review and meta-analysis. *Front Med (Lausanne)*. 2020;7:549. doi: [10.3389/fmed.2020.00549](https://doi.org/10.3389/fmed.2020.00549).
- [46] Bosco A, Almeida B, Pereira P, et al. The uremic toxin methylguanidine increases the oxidative metabolism and accelerates the apoptosis of canine neutrophils[J]. *Vet Immunol Immunopathol*. 2017;185:14–19. doi: [10.1016/j.vetimm.2017.01.006](https://doi.org/10.1016/j.vetimm.2017.01.006).
- [47] Gil R, Ortiz A, Sanchez-Niño M, et al. Increased urinary osmolyte excretion indicates chronic kidney disease severity and progression rate. *Nephrol Dial Transplant*. 2018;33(12):2156–2164. doi: [10.1093/ndt/gfy020](https://doi.org/10.1093/ndt/gfy020).
- [48] Nallu A, Sharma S, Ramezani A, et al. Gut microbiome in chronic kidney disease: challenges and opportunities. *Transl Res*. 2017;179:24–37. doi: [10.1016/j.trsl.2016.04.007](https://doi.org/10.1016/j.trsl.2016.04.007).
- [49] Vanholder R, Glorieux G. The intestine and the kidneys: a bad marriage can be hazardous. *Clin Kidney J*. 2015;8(2):168–179. doi: [10.1093/ckj/sfv004](https://doi.org/10.1093/ckj/sfv004).
- [50] Ren Z, Fan Y, Li A, et al. Alterations of the human gut microbiome in chronic kidney disease. *Adv Sci (Weinh)*. 2020;7(20):2001936. doi: [10.1002/advs.202001936](https://doi.org/10.1002/advs.202001936).
- [51] Aronov P, Luo F, Plummer N, et al. Colonic contribution to uremic solutes. *J Am Soc Nephrol*. 2011;22(9):1769–1776. doi: [10.1681/ASN.2010121220](https://doi.org/10.1681/ASN.2010121220).
- [52] Dubin R, Rhee E. Proteomics and metabolomics in kidney disease, including insights into etiology, treatment, and prevention. *Clin J Am Soc Nephrol*. 2020;15(3):404–411. doi: [10.2215/CJN.07420619](https://doi.org/10.2215/CJN.07420619).
- [53] Peters J. Tryptophan nutrition and metabolism: an overview. *Adv Exp Med Biol*. 1991;294:345–358. doi: [10.1007/978-1-4684-5952-4_32](https://doi.org/10.1007/978-1-4684-5952-4_32).
- [54] Keszthelyi D, Troost F, Masclee A. Understanding the role of tryptophan and serotonin metabolism in gastrointestinal function. *Neurogastroenterol Motil*. 2009;21(12):1239–1249. doi: [10.1111/j.1365-2982.2009.01370.x](https://doi.org/10.1111/j.1365-2982.2009.01370.x).
- [55] Roager H, Licht T. Microbial tryptophan catabolites in health and disease. *Nat Commun*. 2018;9(1):3294. doi: [10.1038/s41467-018-05470-4](https://doi.org/10.1038/s41467-018-05470-4).
- [56] O'mahony S, Clarke G, Borre Y, et al. Serotonin, tryptophan metabolism and the brain-gut-microbiome axis. *Behav Brain Res*. 2015;277:32–48. doi: [10.1016/j.bbr.2014.07.027](https://doi.org/10.1016/j.bbr.2014.07.027).
- [57] Yacoub R, Wyatt C. Manipulating the gut microbiome to decrease uremic toxins. *Kidney Int*. 2017;91(3):521–523. doi: [10.1016/j.kint.2017.01.003](https://doi.org/10.1016/j.kint.2017.01.003).
- [58] Chen Y, Chen D, Chen L, et al. Microbiome-metabolome reveals the contribution of gut-kidney axis on kidney disease. *J Transl Med*. 2019;17(1):5. doi: [10.1186/s12967-018-1756-4](https://doi.org/10.1186/s12967-018-1756-4).
- [59] Koppe L, Mafra D, Fouque D. Probiotics and chronic kidney disease. *Kidney Int*. 2015;88(5):958–966. doi: [10.1038/ki.2015.255](https://doi.org/10.1038/ki.2015.255).
- [60] Schulman G, Berl T, Beck G, et al. The effects of AST-120 on chronic kidney disease progression in the United States of America: a post hoc subgroup analysis of randomized controlled trials. *BMC Nephrol*. 2016;17(1):141. doi: [10.1186/s12882-016-0357-9](https://doi.org/10.1186/s12882-016-0357-9).
- [61] Devlin A, Marcobal A, Dodd D, et al. Modulation of a circulating uremic solute via rational genetic manipulation of the gut microbiota. *Cell Host Microbe*. 2016;20(6):709–715. doi: [10.1016/j.chom.2016.10.021](https://doi.org/10.1016/j.chom.2016.10.021).
- [62] Wang Y, Li J, Chen C, et al. Targeting the gut microbial metabolic pathway with small molecules decreases uremic toxin production. *Gut Microbes*. 2020;12(1):1–19. doi: [10.1080/19490976.2020.1823800](https://doi.org/10.1080/19490976.2020.1823800).